

A Novel Energy Measurement System for the OMEGA Laser

Target experiments conducted using the OMEGA laser system will require an on-target, beam-to-beam UV energy balance of 3%–4%. As a prerequisite, we have implemented an accurate beam-energy diagnostic system. This system is capable of measuring the UV laser energy and the residual green and IR energies of all 60 beams with a relative beam-to-beam accuracy of a fraction of a percent.

Overview of the Harmonic Energy Diagnostic (HED)

The stringent requirements imposed on the harmonic energy diagnostic (HED) system stimulated the adoption of a novel approach that is fundamentally different from the system implemented previously on the 24-beam OMEGA laser (see Fig. 63.14). The only common element is the use of integrating spheres that sample fractions of all three wavelengths emerging from the frequency-conversion crystals. The previous

system [Fig. 63.14(a)] used discrete PIN diode detectors, with colored glass filter stacks, to isolate and sample the wavelengths of interest. The electrical signals generated by these detectors were carried by long triax cables to a central diagnostic location where they were digitized and processed by a computer. It was generally accepted that this measurement technique would be too expensive and not sufficiently precise for the 60-beam system. In the new approach [Fig. 63.14(b)] a fiber-optic delivery system coupled to a CCD detector array is used. Fibers carry the light at all three wavelengths from the integrating spheres, one per beamline, to a common location for measurement. By separating each wavelength at the output end of these fibers, only one fiber is required for each sphere, thus reducing the number of components. Furthermore, by separating the wavelengths for all the fiber-optic outputs simultaneously, the fiber outputs can be optically coupled to a

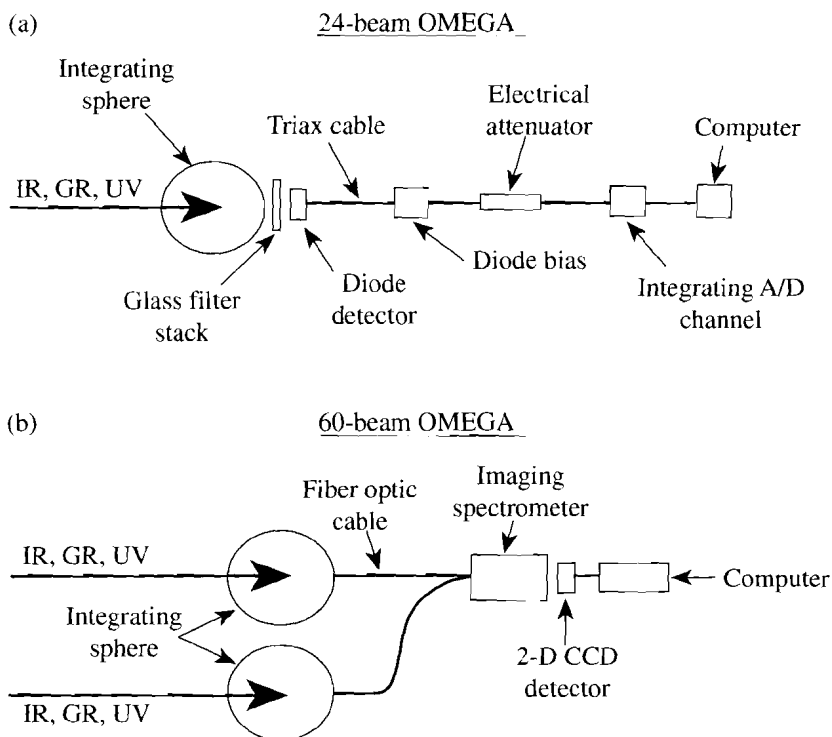


Fig. 63.14

Techniques used for laser-energy measurement on (a) the original, 24-beam OMEGA system and (b) the upgraded, 60-beam system. In the original system PIN photodiode detectors looked into an integrating sphere through three filter stacks, one for each wavelength (IR, green, and UV), and the signals were transmitted electrically to a computer. In the new system, a 300- μm -diam optical fiber samples the three wavelengths at each integrating sphere and is connected to one of two imaging spectrometers. The images are read out by a CCD detector.

E7664

single, large-format, two-dimensional CCD array detector. This architecture eliminates the need for individual detectors and acquisition channels.

Within each stage-F alignment sensor package (F-ASP) there is a three-wavelength energy pickoff, one for each beamline. The optical system is shown schematically in Fig. 63.15. The pickoff is a wedged, full-aperture piece of fused silica that is tilted at 5° to the incoming beam. The surfaces of the pickoff are curved, with radii chosen to produce a net optical power of zero in transmission. The first surface is uncoated and provides a Fresnel reflection of $\sim 4\%$ for each of the three wavelengths. The second surface is antireflection coated; approximately 0.5% of the beam energy is reflected from this surface but, because of the wedge, this reflection is prevented from entering the integrating sphere (see below). A second $\sim 4\%$ reflection occurs from a 5-in.-diam flat wedge, also made of fused silica and also tilted at 5° . The beam then passes through a window into a vacuum tube, through focus, and through a lens that recollimates it at a diameter of 36 mm before it enters the integrating sphere. A 2-in. disk of Spectralon^{TM1} (sintered Teflon, a highly diffusing material with a high damage threshold) is placed in the directly irradiated portion of the integrating sphere. The remainder of the sphere is painted on the inside with BaSO₄.

The second wedge is uncoated and serves two purposes. First, it attenuates the beam energy to 0.16% of its initial value to avoid damaging the inside of the integrating sphere. Second, it is tilted in the orthogonal plane to that of the first wedge so that the net attenuation of both wedges is the same for both “s” and “p” polarizations; this is important because the polarization of the residual IR is indeterminate. The vacuum tube is used to avoid air breakdown in the vicinity of focus, where a knife edge eliminates reflections off the second surface of each wedge. (Both wedges are in the same plane.) Laser energy

transmitted through the second wedge is absorbed by a piece of 19-mm-thick filter glass. The optical design ensures that the integrating sphere is located at a system image relay plane. Thus, if co-propagation² is added to the system, the main and foot pulses will be spatially separated at the rear of the integrating sphere. A second sphere will then be added to diagnose the foot pulse.

The energy in each integrating sphere is sampled using a large-core, 300- μm -diam, silica optical fiber. These fibers are routed through dedicated fiber-optic conduits that protect the fibers and make them less susceptible to bending-radius changes caused by incidental touching or bumping during routine system maintenance. (Changing the bending radius changes the transmission through the optical fiber.³) The fibers are bundled in an ordered array of rows and columns and connected to the input of the HED measurement system. This is a spectrometer that images the output ends of all fibers onto a single CCD detector. The dispersion of the spectrometer provides for the formation of three discrete images of each fiber, one for each wavelength (see Fig. 63.16). The integrated intensity of each image is proportional to the energy in the associated beamline at the selected wavelength. The constant of proportionality is obtained from cross-calibration with conventional full-energy, full-aperture absorption calorimeters. These calorimeters are located at the output of the F-ASP structures and are rotated into the beamlines when recalibration is required. These calorimeters provide absolute energy calibration at each wavelength for each beamline.

Integrating Sphere

Significant measurement errors due to speckle can result when sampling coherent light from an integrating sphere. These errors originate from natural shot-to-shot pointing and wavefront variations in the laser output and occur when the number of speckles incident on the detector, or fiber in this

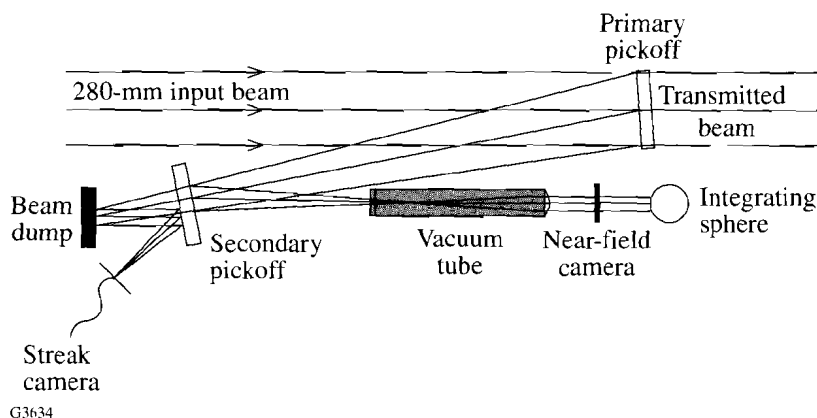


Fig. 63.15
Optical layout within the stage-F alignment sensor package (F-ASP). A small fraction of the energy in each beam is split off by the combination of a curved primary pickoff and a flat, wedged secondary pickoff and down-collimated to a 6-in.-diam integrating sphere.

G3634

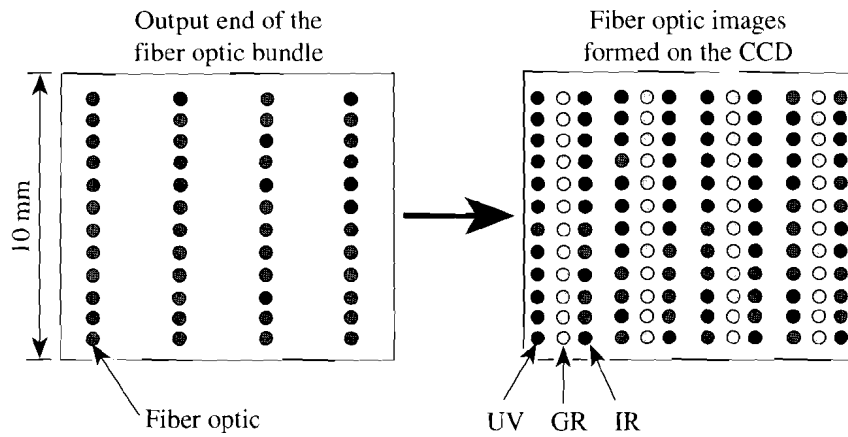
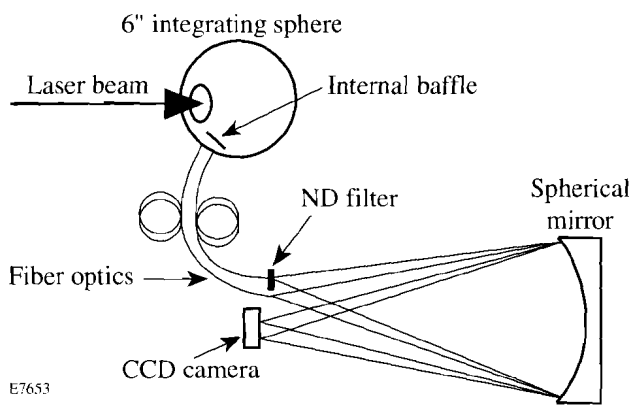


Fig. 63.16
Schematic of the output end of one of the two fiber-optic bundles (left). Each 300- μm fiber is shown as a dark circle. The spectrometer images this 10-mm-square bundle onto the CCD array as shown on the right, creating three images of each fiber, one for each wavelength. There are 96 inputs for each spectrometer. Of the 48 inputs shown, 30 are used for beam-energy measurements.

E7532

case, is small enough to produce poor sampling statistics. In the HED implementation, the 300- μm -diam fiber was tested to determine if it was compatible with the performance requirements of this instrument. A prototype integrating sphere and fiber-optic system were set up for this purpose. Two fibers were attached at different points to this sphere and imaged onto a single CCD detector (see Fig. 63.17). The sphere was illuminated with coherent light from a pulsed laser system, and the ratio of the signals from the fiber images on the CCD was recorded. The ratio of the two CCD signals remained constant, indicating that the detection system was insensitive to changes in the speckle pattern.

The linearity of the CCD detector response was tested over four orders of magnitude for short-pulse (<1-ns) signals in the IR, the green, and the UV. The same setup as Fig. 63.17 was used for this purpose, with one of the two fiber outputs attenuated by a factor of 5 relative to the other fiber using neutral density filters at the output of the fiber. The intensity ratio of the two images remained constant within a small but measurable deviation (see Fig. 63.18). A better fit was obtained by assuming that the CCD signal S was of the form $S = aE + bE^2$, where E is the optical input signal. Best fits for the coefficients a and b were found for the operating range of interest (a relative input signal in the range of 0.1–1.0) as

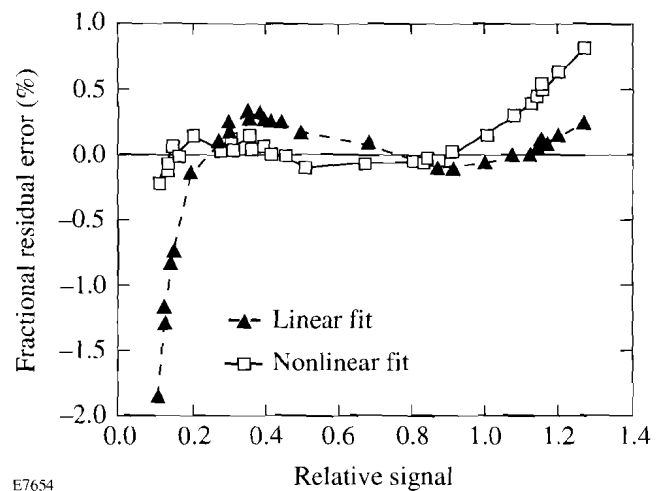


E7653

Fig. 63.17
Setup for determining the energy measurement sensitivity to speckle. Two fibers are linked to one integrating sphere and imaged onto the same CCD array. The ratio of the two CCD images remains constant from shot to shot, indicating insensitivity to changing speckle patterns.

CCD Detector

Considerable testing of the detection system (integrating sphere, fiber, spectrometer, and CCD array) was carried out to establish its efficacy in terms of both performance and cost.



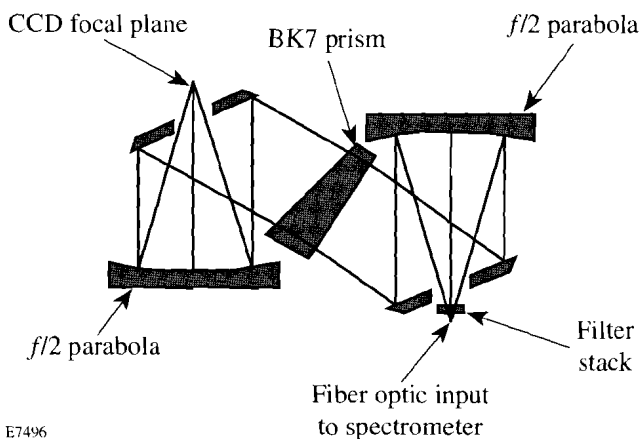
E7654

Fig. 63.18
Results from a linearity test on the CCD array. Two signals were imaged onto the CCD array, as in Fig. 63.17, but with one signal attenuated by a factor of 5. Deviations of the ratio of measured signals from this factor are plotted on the vertical axis assuming a linear fit (dashed curve) and a nonlinear fit that corrects for deviations from linearity using a small quadratic term (solid curve). The quadratic term is a fraction 0.027 of the linear term at a relative signal of 1.0. The nonlinear fit is optimized for relative signals in the range 0.1–1.0.

shown in Fig. 63.18, which illustrates the linear and nonlinear fits for the UV wavelength. The residual error corresponding to the nonlinear fit represented a very small ($\sim 0.2\%$) overall measurement error that can remain uncorrected. The nonlinear correction is in fact not strictly necessary for beam energy balance since all beams are equally affected by the small nonlinearity, which is only 2.7% at the maximum optical energy E (i.e., $bE/a = 0.027$ at this point). Figure 63.18 also validates the speckle-insensitive nature of the HED detection system.

Optical Design of the HED Spectrometer

The spectrometer for the HED energy measurement system is designed to match the characteristics of the fiber-optic input bundle, the CCD array, and the imaging system. The HED system is a low-dispersion instrument with fast ($f/1.6$) optics that match the numerical aperture of the fibers in the ultraviolet for maximum collection efficiency. The fiber-optic bundle does not need to be imaged near the diffraction limit of the $f/1.6$ system since it is sufficient for the light from each fiber in the bundle to be collected and concentrated into a confined spot. In fact, 50 times diffraction-limited performance (50 XDL) is sufficient to concentrate all the light into a circle of diameter less than $500\ \mu\text{m}$ at the detector, allowing large amounts of astigmatism, coma, and field curvature to be tolerated. This permitted a cost-effective, all-reflective spectrometer design using parabolic mirrors. An on-axis Pfund⁴ parabolic system using flat mirrors with central holes in combination with the parabolic mirrors was selected (Fig. 63.19). The parabolic mirrors were diamond turned to a



E7496

Fig. 63.19

Optical design of the HED spectrometer. This is based on Pfund's use of plane mirrors with central openings to avoid astigmatism when using parabolic collimating and focusing elements. A BK7 prism is used as the dispersive element. A single glass filter stack is used at the input to attenuate the IR, green, and UV light from each fiber.

figure tolerance of half a wave and then post-polished to remove the grooves. After post-polishing, the final figure of the parabolas deviated by as much as two waves, which was well within the specifications for the HED application. This loose surface figure specification made the post-polishing step easy and cost effective. Additionally, the post-polishing ensured a final surface roughness of less than $5\ \text{\AA}$ rms. All mirror surfaces have protected, enhanced UV aluminum coatings with insignificant reflective losses. Scattered light due to the central hole in the flat pickoff mirrors is minimal. Ray-trace evaluation determined that the fiber images, although heavily aberrated, especially at the edge of the field, concentrated the light into well-defined regions on the detector. An example of a digitized CCD image of a single fiber is shown in Fig. 63.20.

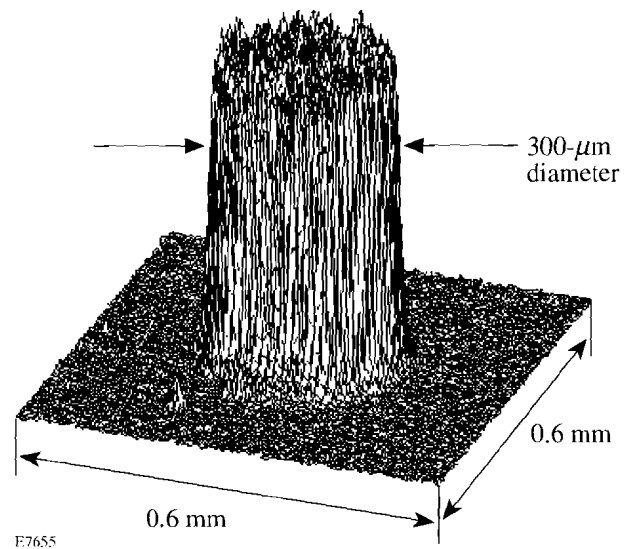


Fig. 63.20

Isometric view of a digitized CCD image of a single fiber from the multifiber bundle as imaged by the spectrometer. The fiber image is well confined within a square region of the array.

The dispersive element chosen for the HED is a single-pass, uncoated, 6° BK7 glass prism, which provides the required dispersion of $\sim 400\ \text{nm/mm}$. Ray-trace analysis determined that multiple-order surface reflections from the prism faces and other reflective surfaces do not reach the detector plane.

To ensure adequate performance of the HED system it was essential to remove the vacuum window from the CCD camera. This was done primarily because this window created a serious reflected-light problem at the detector surface (see Fig. 63.21). The CCD array surface is reflective, allowing the converging light cone that focuses on this surface to be reflected back to the input vacuum window. This reflection, which is now diverg-

ing, is reflected back to the CCD detector surface by the window, showing up as a halo of light around the initial focal spot. The multiple reflections supported by this geometry result in the signal being spread for several millimeters across the detector surface. A three-wavelength antireflection coating for the window would have at best a reflectivity of a few tenths of 1% from each surface, and the image quality would still be spoiled. Tilting the window enough to walk the reflections off the array would introduce significant astigmatism. Operating the CCD camera without a vacuum window requires purging of the spectrometer with dry nitrogen (at 1 psi above ambient pressure) to protect the cooled CCD array from the condensation of atmospheric moisture. This requirement significantly affected the mechanical design of the spectrometer housing.

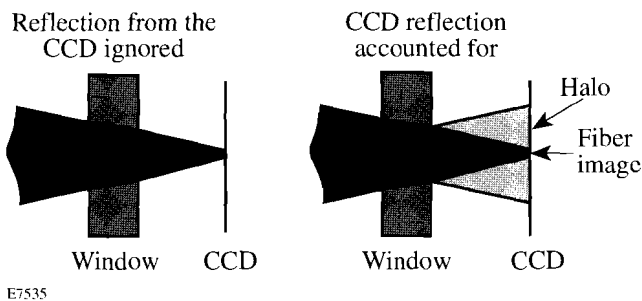


Fig. 63.21

Influence of the CCD camera window on image quality. The converging cone of light rays is focused on the CCD plane (left). With a window, some light is reflected from the CCD surface (right) and back from the window onto the CCD, leading to a halo around the image and errors in the energy measurement.

Mechanical Design of the HED Spectrometer

The primary considerations for the HED spectrometer enclosure were mechanical stability, operational simplicity, and nitrogen purging. These considerations ruled out some designs found in several commercially available spectrometers. For example, some larger spectrometers used a thick, flat mounting plate for the optical elements and a light-tight, sheet-metal cover, but this design would have been hard to seal and maintain at a positive pressure. Ray-trace analysis showed that the 50 XDL imaging requirement results in tolerances in the range of milliradians and hundreds of microns. Thus it was sufficient to machine optical mounting stations directly into the spectrometer housing without any positioning adjustments, allowing the spectrometer housing to be fabricated from solid blocks of aluminum. The housing is rigid and stable and contains the HED optics folded into a compact 20-in. \times 16-in. \times 9-in. package. A photograph of the spectrometer is shown in

Fig. 63.22. The only adjustable component in the system is the mount for the fiber-optic bundle. This mount allows for x , y , z , and θ motion for proper centering, focusing, and angular orientation of the images on the CCD. O-ring gaskets are used to seal the spectrometer, allowing for the 1-psi overpressure and a small flow of dry nitrogen.

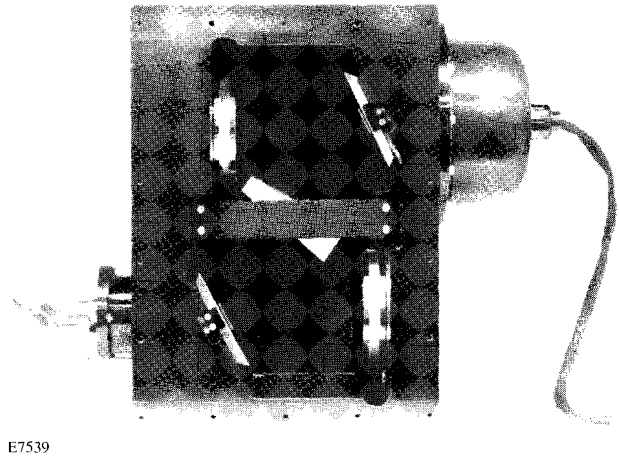


Fig. 63.22

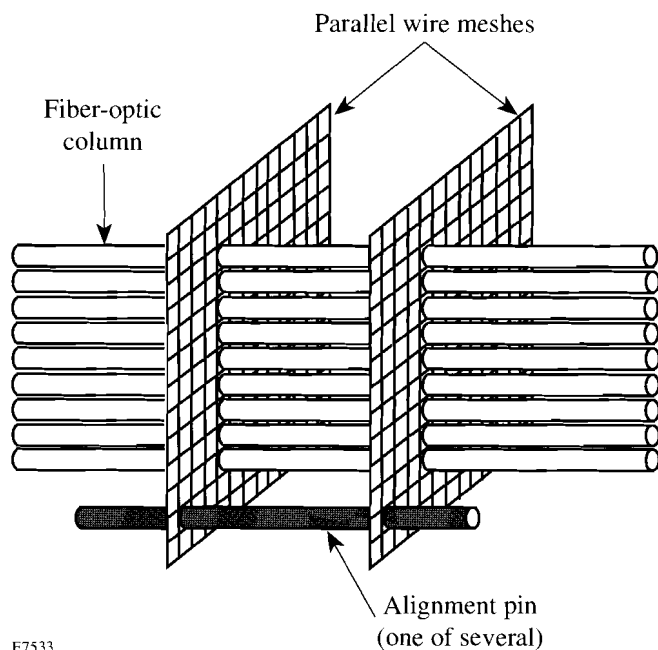
View of the imaging spectrometer, showing the interior cavity that has been hollowed out from a solid block of aluminum. The optical elements (two parabolic mirrors, two flat mirrors, and a prism) are viewed edge-on. The fiber-optic bundle is inserted into the port on the upper right side. The CCD camera is mounted on the lower left side with the array behind the flat mirror. A gasketed plate is used to cover the front.

Multichannel Fiber-Optic Input Bundle

Fabrication of the 96-fiber bundle (300- μm core diameter) presented some challenge. This number of fibers was needed to accommodate 30 (three-color) input channels for UV conversion measurements, 30 channels for passive IR beam-balance measurements (taken from flip-in pickoffs in the final, stage-F spatial filters), and several spare channels. At the other end of the bundle each fiber terminates with a fiber-optic patch panel. Each fiber in the bundle is 1 m long.

The fiber-bundle array facing the HED spectrometer is arranged in eight columns of 12 fibers (see Fig. 63.23). Each fiber must be held at a precise transverse location within the bundle. Only the rotation of the fiber-optic core relative to the optical axis of the fiber is uncontrolled—and unimportant. To ensure that the image of each fiber optic reaches the CCD detector within a few pixels of the desired location, the horizontal and vertical position tolerance of each fiber within the

bundle is $50\ \mu\text{m}$. The tip-tilt angle of the fiber relative to the output surface normal is held to better than 2 mrad to prevent signal loss and unnecessary scattering of light due to miscentering on the clear aperture of the spectrometer imaging optics. Finally, all fibers must be in the same plane to within $25\ \mu\text{m}$ to ensure that the image from each fiber is focused at the detector surface.



E7533

Fig. 63.23

Wire meshes used to hold the fiber bundle in position. Metal alignment pins around the perimeter (one shown) support the meshes. Nine fibers from a column are shown; the mesh holds 96 fibers in total (8 columns of 12).

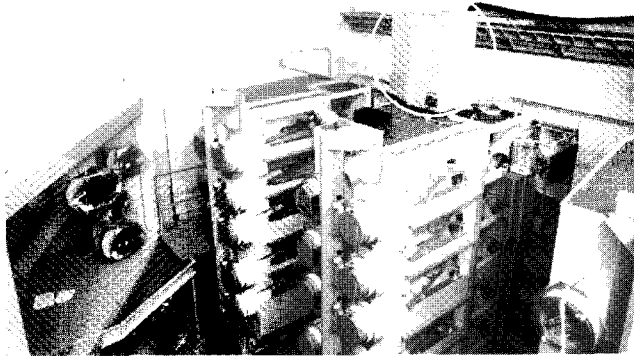
This precision is achieved using two parallel wire meshes spaced 8 mm apart (Fig. 63.23). The wire meshes are coated with 5 to $10\ \mu\text{m}$ of parylene prior to insertion of the fibers to prevent scratching of the fibers. The pitch and wire diameter of the mesh are selected such that the outer diameter of the fiber-optic plastic buffer fits tightly into the mesh opening. The wire meshes are cut into 25-mm squares and secured with several pins around the perimeter. Before inserting the fibers into the mesh assembly, a 10-mm length of the plastic buffer is removed (to prevent interference with the subsequent polishing operation), exposing the glass-clad core of the fiber.

During the assembly process, each fiber is inserted such that the plastic buffer extends a few millimeters beyond the second mesh. After insertion, each column of 12 fibers is held in position with a small amount of fast-curing epoxy. After all

eight columns are in place, an enclosure around the fibers and the supporting mesh is filled with epoxy. The selected epoxy is one that cures with minimal shrinkage, is opaque from the IR to the UV, and can be coarse ground and polished. In addition, it has a low viscosity and is slow curing in order to fill in the spaces between the fibers and the supporting mesh and allow trapped air to escape. Once the epoxy is fully cured, the forms are removed and the exposed epoxy block is ground into a 1-in.-long, 5/8-in.-diam, cylindrical shape. The fiber output end is then coarse ground until all 96 fibers are exposed. A 3/4-in.-diam stainless steel tube with 1/32-in.-thick walls is slid over this epoxy rod such that the output end of the epoxy assembly extends about 1/8 in. beyond the end of the stainless steel tube. Additional epoxy is used to fill the gap between the epoxy rod and the stainless steel tube. Once cured, the output end of this assembly is fine ground and polished. A 3-in.-diam, 1/2-in.-thick aluminum disk with a 3/4-in.-diam hole for the bundle to slide into ensures that the output face of the bundle is ground flat. All work is done using a figure-eight rubbing motion under a steady stream of cold water. Approximately two hours of polishing with abrasive grit sizes ranging from $30\ \mu\text{m}$ to $0.3\ \mu\text{m}$ produces a polished bundle free of any scratched or cracked fiber-optic ends when viewed under an optical microscope.

Installation of the HED System

Fully assembled, each HED spectrometer, together with its supporting electronics and utilities, weighs about 300 lbs. Half the weight is due to the spectrometer housing, with the remaining weight due to the steel enclosure, power supplies, and CCD cooling units. Each system is housed in an EMI-shielded rack and placed on top of an F-ASP structure (see Fig. 63.24). The optical fibers from the integrating spheres are connected to the patch panels on the enclosures. A 70-psi dry nitrogen line, a fiber-optic communications connection to the remote computer network, a 120-V ac power feed, and an RG58 coax cable from the timing system are all connected to the HED unit. A trigger signal is provided by the timing system 10 s before the laser system fires so the HED can initiate internal preshot preparations. These preparations include blanking the CCD array to ensure that any residual charge has been cleared from each pixel before new data is taken. The spectrometer shutter is opened from 25 ms prior to a laser shot to 25 ms after the shot to ensure capture of the images on the CCD array. The CCD frame is later transferred from the HED unit via a computer network to the data acquisition, analysis and archiving computers. These computers reduce the data to determine the energies and conversion efficiencies and the beam-to-beam energy balance.



E7540

Fig. 63.24

HED enclosure shown inside the white circle on top of the F-ASP structure. The fiber optics are routed from each integrating sphere, through the square conduits, to the back of the HED rack.

Conclusion

The harmonic energy diagnostic (HED) is now an integral part of the OMEGA laser system. Data collected by the HED has been used to perform on-line, high-power, fine tuning of the frequency-conversion crystals for the 60-beam system. In

addition, the HED system has provided the energy measurements used to confirm that the laser system meets its output-energy and beam-to-beam energy-balance acceptance specifications. In the future the HED, together with other instrumentation, will provide crucial measurements needed to improve the on-target energy balance.

ACKNOWLEDGMENT

This work was supported by the U.S. Department of Energy Office of Inertial Confinement Fusion under Cooperative Agreement No. DE-FC03-92SF19460, the University of Rochester, and the New York State Energy Research and Development Authority. The support of DOE does not constitute an endorsement by DOE of the views expressed in this article.

REFERENCES

1. "Spectralon" is a proprietary product available from Labsphere, N. Sutton, NH 03260.
2. R. S. Craxton, ed., *OMEGA Upgrade Preliminary Design*, Laboratory for Laser Energetics Report DOE/DP 40200-101, University of Rochester (1989).
3. A. A. P. Boechat *et al.*, *Appl. Opt.* **30**, 321 (1991).
4. R. A. Sawyer, *Experimental Spectroscopy*, 3rd ed. (Dover Publications, NY, 1963).